Isolation and characterization of NY-ESO-1–specific T cell receptors restricted on various MHC molecules

Michael T. Bethune[a,1], Xiao-Hua Li[b,1], Jiaji Yu[b,c,1], Jami McLaughlin[b], Donghui Cheng[b], Colleen Mathis[b], Blanca Homet Moreno[d], Katherine Woods[e,f,g], Ashley J. Knights[g], Angel Garcia-Diaz[d], Stephanie Wong[a], Siwen Hu-Lieskovan[d], Cristina Puig-Saus[d], Jonathan Cebon[e,f,g], Antoni Ribas[d,h,i,j,k], Lili Yang[b,h,i,j,2], Owen N. Witte[b,h,k,2], and David Baltimore[a,2]

[a]Division of Biology and Biological Engineering, California Institute of Technology, Pasadena, CA 91125; [b]Department of Microbiology, Immunology, and Molecular Genetics, University of California, Los Angeles, CA 90095; [c]Molecular Biology Institute, University of California, Los Angeles, CA 90095; [d]Division of Hematology and Oncology, Department of Medicine, University of California, Los Angeles, CA 90095; [e]Cancer Immunobiology Laboratory, Olivia Newton-John Cancer Research Institute, Austin Hospital, Heidelberg, VIC 3084, Australia; [f]School of Cancer Medicine, La Trobe University, Bundoora, VIC 3086, Australia; [g]Cancer Immunobiology Laboratory, Ludwig Institute for Cancer Research, Heidelberg, VIC 3084, Australia; [h]Eli and Edythe Broad Center of Regenerative Medicine and Stem Cell Research, University of California, Los Angeles, CA 90095; [i]Jonsson Comprehensive Cancer Center, University of California, Los Angeles, CA 90095; [j]Department of Medicine, University of California, Los Angeles, CA 90095; and [k]Parker Institute for Cancer Immunotherapy, University of California, Los Angeles, CA 90095

Tumor-specific T cell receptor (TCR) gene transfer enables specific and potent immune targeting of tumor antigens. Due to the prevalence of the HLA-A2 MHC class I supertype in most human populations, the majority of TCR gene therapy trials targeting public antigens have employed HLA-A2–restricted TCRs, limiting this approach to those patients expressing this allele. For these patients, TCR gene therapy trials have resulted in both tantalizing successes and lethal adverse events, underscoring the need for careful selection of antigenic targets. Broad and safe application of public antigen-targeted TCR gene therapies will require (i) selecting public antigens that are highly tumor-specific and (ii) targeting multiple epitopes derived from these antigens by obtaining an assortment of TCRs restricted by multiple common MHC alleles. The canonical cancer-testis antigen, NY-ESO-1, is not expressed in normal tissues but is aberrantly expressed across a broad array of cancer types. It has also been targeted with A2-restricted TCR gene therapy without adverse events or notable side effects. To enable the targeting of NY-ESO-1 in a broader array of HLA haplotypes, we isolated TCRs specific for NY-ESO-1 epitopes presented by four MHC molecules: HLA-A2, -B07, -B18, and -C03. Using these TCRs, we pilot an approach to extend TCR gene therapies targeting NY-ESO-1 to patient populations beyond those expressing HLA-A2.

NY-ESO-1 | immunotherapy | T cell receptor gene therapy | TCR | MHC

The αβ T cell receptor (TCR) determines the unique specificity of each nascent T cell. Upon assembly with CD3 signaling proteins on the T cell surface, the TCR surveils peptide ligands presented by MHC molecules on the surface of nucleated cells. The specificity of the TCR for a peptide–MHC complex is determined by both the presenting MHC molecule and the presented peptide. The MHC locus (also known as the HLA locus in humans) is the most multiallelic locus in the human genome, comprising >18,000 MHC class I and II alleles that vary widely in frequency across ethnic subgroups (1, 2). Ligands presented by MHC class I molecules are derived primarily from proteasomal cleavage of endogenously expressed antigens. Infected and cancerous cells present peptides that are recognized by CD8⁺ T cells as foreign or aberrant, resulting in T cell-mediated killing of the presenting cell.

T cells can be engineered to kill tumor cells through the transfer of tumor-reactive αβ TCR genes (3). Key to this approach is that the patient expresses the MHC allele on which the therapeutic TCR is restricted and that the targeted peptide is derived from a tumor-associated or tumor-specific antigen. Private (patient-specific) neoantigens resulting from tumor-specific mutations are a potential source of such targets (4). However, implementation of personalized TCR gene therapy is complicated by the need to identify mutations through sequencing, to isolate mutation-reactive, patient-specific TCRs, and to genetically modify patient T cells on demand. This is still more challenging for tumors that cannot be accessed for sequencing and for low-mutational-burden tumors with few or no neoantigens (5). Particularly for these last tumor types, targeting public, tumor-restricted antigens with off-the-shelf TCRs remains an attractive option.

The first public antigen targeted with TCR gene therapy in the clinic was melanocyte antigen MART1/Melan-A, yielding objective responses in 2/15 patients with metastatic melanoma (6). Use of a higher-affinity MART1-reactive TCR (F5) increased the response rate to 30% but also engendered vitiligo, uveitis, and transient hearing loss due to MART1 expression on healthy

Significance

T immune cells can be engineered to express tumor-specific T cell receptor (TCR) genes and thereby kill cancer cells. This approach—termed TCR gene therapy—is effective but can cause serious adverse events if the target is also expressed in healthy, noncancerous tissue. NY-ESO-1 is a tumor-specific antigen that has been targeted successfully and safely through TCR gene therapies for melanoma, synovial sarcoma, and myeloma. However, trials to date have focused exclusively on a single NY-ESO-1–derived epitope presented on HLA-A*02:01, limiting application to patients expressing that allele. In this work, we isolate TCRs that collectively recognize multiple NY-ESO-1–derived epitopes presented by multiple MHC alleles. We thereby outline a general approach for expanding targeted immunotherapies to more diverse MHC haplotypes.

melanocytes in the skin, eye, and middle ear (7). T cell therapies targeting other public antigens have similarly engendered morbidity or serious adverse events due to on-target/off-tumor reactivity. Targeting carcinoembryonic antigen produces severe colitis in patients with metastatic colorectal cancer due to reactivity with normal colorectal tissue (8). More seriously, T cell therapies targeted at ERBB2 or MAGE-A3 each resulted in deaths due to unappreciated expression of the target antigen (or similar variant) on vital organs (9, 10). Thus, these studies underscore the importance of identifying stringently tumor-specific public antigens (11), particularly when well-expressed, high-affinity targeting receptors necessary for therapeutic success are employed (7, 12).

NY-ESO-1—the product of the *CTAG1B* gene—is an attractive target for off-the-shelf TCR gene therapy. As the prototypical cancer-testis antigen, NY-ESO-1 is not expressed in normal, nongermline tissue, but it is aberrantly expressed in many tumors (13). The frequency of aberrant expression ranges from 10 to 50% among solid tumors, 25–50% of melanomas, and up to 80% of synovial sarcomas (13–18), with increased expression observed in higher-grade metastatic tumor tissue (14, 15, 19). Moreover, NY-ESO-1 is highly immunogenic, precipitating spontaneous and vaccine-induced T cell immune responses against multiple epitopes presented by various MHC alleles (20–23). As a result, the epitope NY-ESO-1$_{157-165}$ (SLLMWITQC) presented by HLA-A*02:01 has been targeted with cognate 1G4 TCR in gene therapy trials, yielding objective responses in 55% and 61% of patients with metastatic melanoma and synovial sarcoma, respectively, and engendering no adverse events related to targeting (24, 25). Targeting this same A2-restricted epitope with lentiviral-mediated TCR gene therapy in patients with multiple myeloma similarly resulted in 70% complete or near-complete responses without significant safety concerns (26). The majority of patients who respond to therapy relapse within months, and loss of heterozygosity at the MHCI locus has been reported as a mechanism by which tumors escape adoptive T cell therapy targeting HLA-A*02:01/NY-ESO-1$_{157-165}$ (27). Thus, NY-ESO-1 is a tumor-specific, immunogenic public antigen that is expressed across an array of tumor types and is safe to target in the clinic but that is susceptible to escape when targeted through a single HLA subtype.

In this work, we had two goals. First, since TCRs of higher strength and affinity are more efficacious, we sought to identify new TCRs that target A2/NY$_{157-165}$ with comparable or better sensitivity than the clinically employed 1G4 TCR. As affinity-enhanced TCRs can be cross-reactive (28–30), we established a protocol for isolating antigen-reactive TCRs directly from patient blood. Two of these TCRs demonstrated comparable or greater sensitivity than 1G4 both in vitro and in vivo in tumor-killing assays. Second, to broaden the clinical utility of NY-ESO-1 as a TCR gene therapy target, we used our isolation protocol to identify TCRs that target NY-ESO-1 epitopes presented by common MHC alleles other than HLA-A*02:01. We propose that targeting multiple NY-ESO-1 epitopes will enable treatment of a larger patient set and may render treatment more robust toward tumor escape.

Results

Expansion and Isolation of NY-ESO-1–Specific T Cell Clones.
We previously reported the presence of T cells reactive with various NY-ESO-1–derived epitopes in the blood of patients with metastatic melanoma (22). To enrich for these reactive T cells, we stimulated expansion of patient peripheral blood mononuclear cells (PBMCs) with a panel of 28 overlapping 18-mers collectively constituting the full NY-ESO-1 protein sequence (Fig. 1*A*). We then restimulated the expanded cells with individual peptides, performed intracellular staining for IFN-γ to determine which peptides drove expansion, and analyzed stimulatory peptides with a predictive algorithm to identify minimal epitopes relevant to each patient's MHC haplotype (31) (Fig. 1*B*). Reactive T cells

were reexpanded in the presence of individual 9–10-mer peptides corresponding to immunostimulatory epitopes (Fig. 1*C*) and sorted via FACS using cognate peptide–MHC tetramers (Fig. 1*D*). The cell lines grown from these single-cell sorts were clonal and reactive with their cognate epitopes (Fig. 1*E*). In total, four cell lines reactive with HLA-A*02:01/NY$_{157-165}$ and four cell lines reactive with epitopes presented by HLA-B and HLA-C alleles were selected for further study.

Cloning and Screening of NY-ESO-1–Specific TCRs.
We cloned paired TCRα and TCRβ genes from sorted single cells using a commercial RT-PCR kit with custom multiplexed primers targeting all human TRAV and TRBV gene segments. The resulting V_α and V_β cDNAs were subcloned into a retroviral vector backbone with either human or murine TCR constant regions (Fig. 2*A*). To verify the specificity of cloned TCRs, we transfected CD3$^+$ HEK 293T cells with each fully human TCR and stained the transfected cells with peptide–MHC dextramer reagents for each of the targeted NY-ESO-1 epitopes (Fig. 2*B*). All four HLA-A2–restricted TCRs exhibited the expected reactivity (Fig. 2*C*). Although analyzed events were gated for similar transfection level, novel TCRs exhibited highly variable dextramer binding. Dextramer binding for the 9D2 TCR was barely discernible from background, whereas the 3A1 TCR exhibited superior dextramer binding compared with the clinically employed 1G4 TCR. Dextramer binding for 4A2 and 5G6 TCRs were intermediate between 9D2 and 1G4.

Additionally, three of four of the TCRs restricted on MHC alleles other than HLA-A2 were verified to bind their targets specifically (Fig. 2*D*). Transfected 293T cells expressing the B7/NY$_{60-72}$-specific 1E4 TCR, the B18/NY$_{88-96}$-specific 2B8 TCR, or the Cw3/NY$_{96-104}$-specific 3C7 TCR each bound their respective dextramers, whereas untransfected cells did not. Cells transfected with the 9G2 TCR—cloned from T cells that were reactive with Cw3/NY$_{92-100}$—did not detectably bind cognate dextramer relative to untransfected cells. A possible reason for this was that HEK 293T cells do not express the CD8 coreceptor. CD8 increases the avidity of the TCR–pMHC interaction by binding to MHCI directly, enabling lower affinity TCRs to engage (32). We therefore included this TCR for further analysis of CD8 dependency in Jurkat T cells.

Functional Characterization of A2-Restricted, NY-ESO-1–Specific TCRs.
The sensitivity of a TCR-transduced T cell is a function of the monomeric affinity of the TCR for its cognate peptide–MHC (K_d ~ 0.1–400 μM) (33) as well as the density of the TCR on the cell surface (12). Transduced TCRs express on the T cell surface at widely varying levels due to variation in the efficiency with which they fold, dimerize, and compete with endogenous TCRs for assembly with limiting CD3 chains (a property termed TCR "strength") (34, 35). Therefore, optimal cytotoxic function of TCR-transduced T cells correlates with TCR affinity and surface expression (3, 12), underscoring the importance of selecting high-affinity, efficiently exported TCRs for gene therapy (7).

As higher-affinity TCR–pMHC interactions are less dependent on CD8 participation, we reasoned that high-affinity TCRs can be identified by comparing dextramer binding of TCR-transduced Jurkat T cells with or without coexpression of CD8. Additionally, because the strength of surface expression for human TCRs can be increased through substitution with murine constant domains (36), we expressed each TCR as a fully human or murinized derivative to assess each TCR's strength. Cells transduced with vehicle only or with a mismatched TCR (MART1-specific F5 TCR) did not exhibit any binding to A2/NY$_{157-165}$ dextramer (Fig. 3 *A* and *B*). By contrast, cells transduced with the well-established 1G4 TCR (K_d = 9.3 μM) (37) bound cognate dextramer whether 1G4 was fully human or murinized, and whether or not CD8 was present. Murinization of
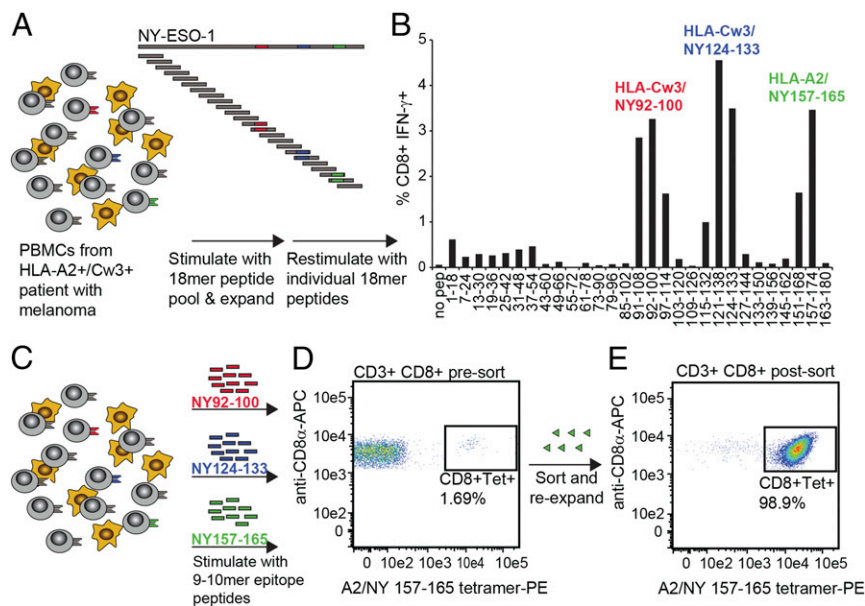
Fig. 1. Expansion and isolation of NY-ESO-1–specific T cell clones. PBMCs were obtained from patients with metastatic melanoma. T cell cloning strategy for a representative HLA-A2+, HLA-Cw3+ donor is shown. (*A*) Schematic outlining the expansion and testing strategy to identify NY-ESO-1–reactive T cell clones. PBMCs were incubated with 28 NY-ESO-1 18-mer peptides (overlapping by 12 aa) and then expanded for 10 d before restimulation with individual peptides in the presence of BFA. Epitopes presented by patient MHC alleles are colored red, blue, and green in those peptides containing the full epitope sequence. (*B*) Representative flow cytometry measurement of intracellular staining for IFN-γ in expanded PBMCs restimulated with individual NY-ESO-1–derived 18-mer peptides. (*C*) Schematic outlining the reexpansion strategy using individual 9–10-mer peptides verified to elicit a T cell response. (*D*) Representative flow cytometry data showing an NY-ESO-1–reactive subpopulation of CD3$^+$CD8$^+$ T cells before sorting. Sorted cells were expanded in the presence of IL-2 and irradiated autologous PBMCs. (*E*) Representative flow cytometry data showing an NY-ESO-1–reactive subpopulation of CD3$^+$CD8$^+$ T cells following sorting.

1G4 increased the intensity of dextramer binding by the muTCR 1.4-fold over the parental huTCR, indicating a modest improvement in strength (Fig. 3 *B* and *C*). The presence of CD8 increased dextramer binding 3.8-fold for 1G4 muTCR. Dextramer binding for TCRs 4A2 and 5G6 was similar in both magnitude and comparative indices to 1G4 (Fig. 3 *A–C*). The 3A1 TCR exhibited only a 1.9-fold increase in dextramer binding in the presence of CD8, indicating that this TCR binds A2/NY$_{157–165}$ with higher affinity than 1G4. This is further supported by the reduced dependence of dextramer binding on CD8 level among CD8$^+$ cells transduced with 3A1 muTCR relative to CD8$^+$ cells transduced with 1G4, 4A2, and 5G6 muTCRs (compare slopes of green populations in Fig. 3*A*). Finally, 9D2 exhibited no detectable binding to dex-

tramer on Jurkat cells in the absence of CD8 and only weak binding upon coexpression of CD8. Murinization of 9D2 did not increase its binding to dextramer.

To compare the functional sensitivity of T cells expressing A2/NY-ESO-1–specific TCRs we coincubated TCR-transduced Jurkat T cells with K562 cells expressing either A*02:01/NY$_{157–165}$ or A*02:01/MART1$_{27–35}$ single-chain trimers (38) and measured secreted IL-2. All TCRs exhibited their expected peptide specificity: The control MART1-specific F5 TCR mediated IL-2 release only in response to MART1 presentation and all NY-ESO-1–specific TCRs mediated IL-2 release only in response to NY-ESO-1 presentation (Fig. 3*D*). Murinization improved functional sensitivity for all TCRs except for 1G4. Consistent with dextramer staining
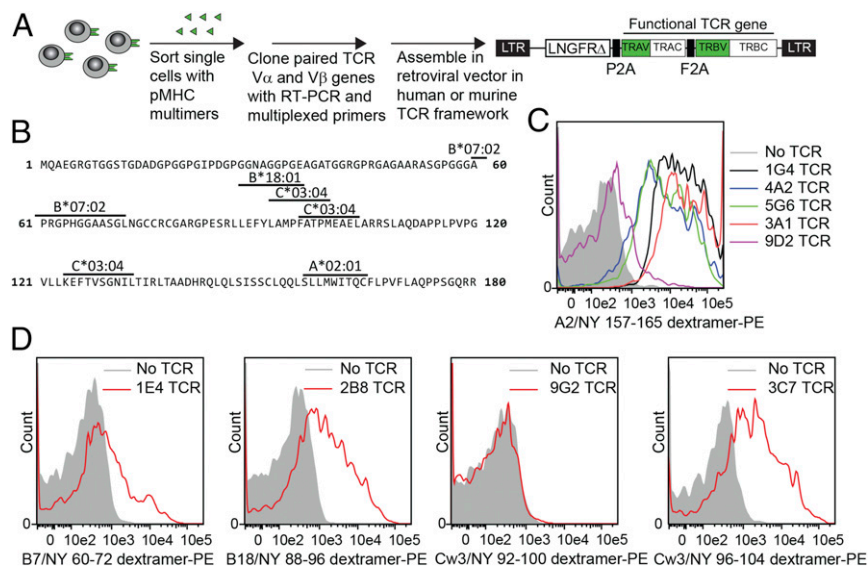
Fig. 2. Cloning and functional screening of NY-ESO-1–specific TCRs. (*A*) Schematic of functional TCR cloning strategy. For each TCR, two constructs were prepared incorporating either human or murine TCR constant domains. (*B*) Protein sequence of NY-ESO-1 with epitopes relevant to this study delineated. (*C*) Flow cytometry histograms comparing HLA-A2/NY$_{157–165}$ dextramer binding by HEK 293T cells transfected with vector backbone only, previously reported 1G4 TCR, and novel A2-restricted, NY-ESO-1–specific TCRs. (*D*) Flow cytometry histograms comparing indicated peptide–MHC dextramer binding by HEK 293T cells transfected with vector backbone only or the indicated novel NY-ESO-1-specificNY-ESO-1–specific TCR restricted on MHC alleles other than HLA-A2. Transfection experiments were performed twice, each in duplicate. Representative histograms are presented.

Fig. 3. Function of A2-restricted, NY-ESO-1–specific TCRs. (*A*) Overlay of representative flow cytometry plots comparing A2/NY$_{157-165}$ dextramer binding by Jurkat and CD8$^+$ Jurkat cells expressing A2-restricted TCRs with human or murine constant domains. (*B*) Dextramer binding mean fluorescence intensity measurements from two independent experiments as in *A*. (*C*) Ratio of dextramer binding mean fluorescent intensity measurements from two independent experiments in *B*. (*D*) ELISA measuring secretion of IL-2 from TCR-transduced Jurkat cells following 48-h coincubation with K562 target cells expressing A2/MART$_{26-35}$ or A2/NY$_{157-165}$ single-chain trimer. Experiment was repeated three times, each with two technical replicates. Means ± SD for a representative experiment are shown. (*E*) ELISA measuring secretion of IFN-γ f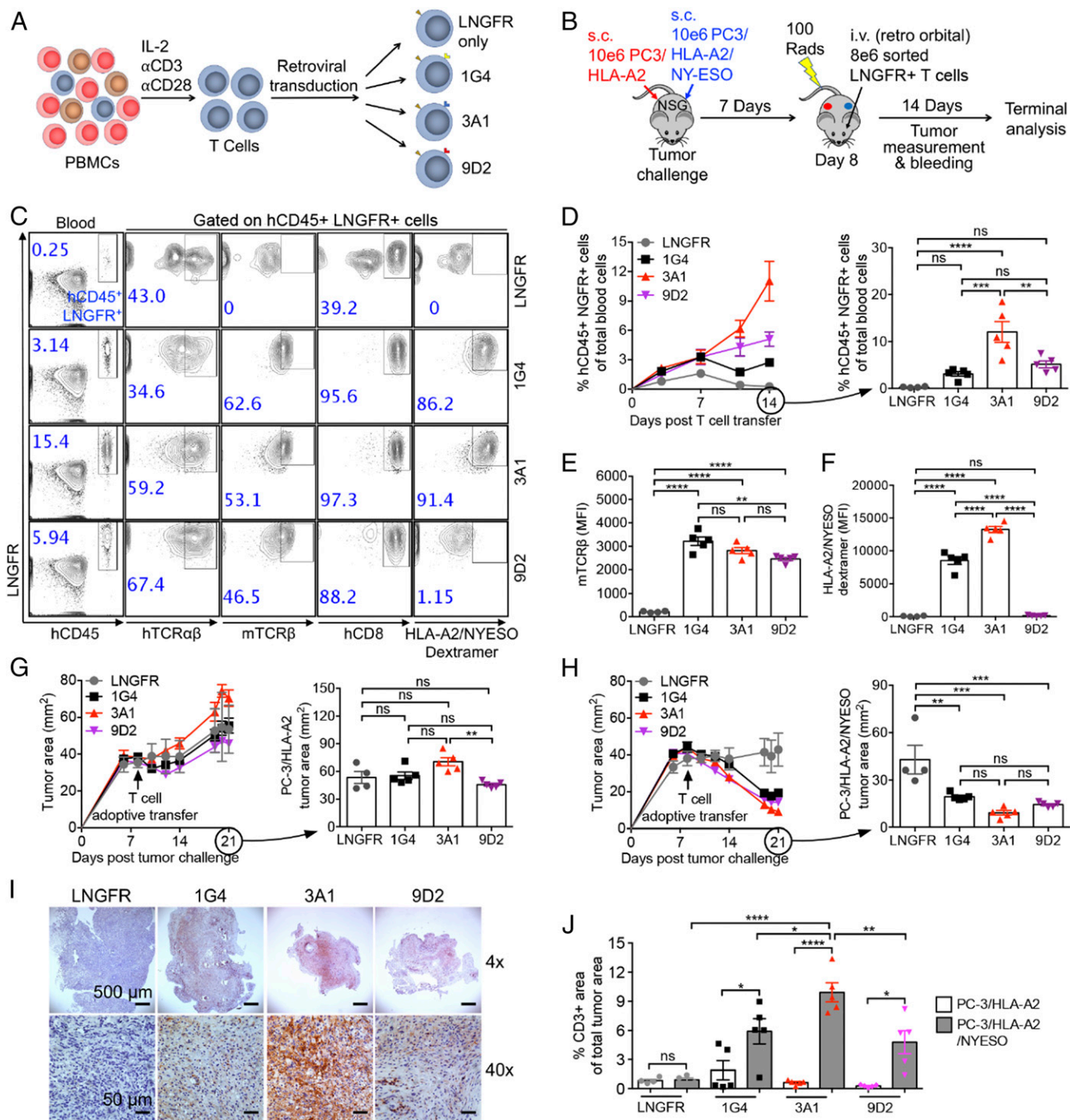rom TCR-transduced PBMCs following 48-h coincubation with the melanoma cell line M257 or an A2$^+$ derivative. Experiment was repeated at least three times, each with two technical replicates. Means ± SD for a representative experiment are shown. (*F*) IncuCyte measurement of total green object area over time as a measurement of TCR-transduced T cell–mediated killing of GFP$^+$ A2$^+$ M257 cells. Means ± SD for four technical replicates are shown.

results, 1G4 and 3A1 muTCRs outperformed 4A2 and 5G6 muTCRs. By contrast, despite its weak binding to dextramer, 9D2 exhibited high functional sensitivity to cognate ligand, comparable to 3A1. To quantify this observation, we pulsed A2$^+$K562 cells with varied concentrations of NY-ESO-1$_{157-165}$ or MART1$_{27-35}$ peptide and then measured IFN-γ secretion from TCR-transduced primary T cells coincubated with peptide-pulsed target cells (*SI Appendix,* Fig. S1 *A* and *B*). As observed with single-chain trimer targets, 3A1, 9D2, and 1G4 exhibited highest sensitivity to NY-ESO-1$_{157-165}$ peptide. The functional sensitivity of 9D2 was 10-fold higher than 4A2, despite 4A2 binding dextramer with 18-fold higher MFI than 9D2 (Fig. 3 *A* and *B*). To evaluate responses to endogenously processed and presented antigen, TCR-transduced primary T cells were coincubated with the human melanoma cell line, A2$^+$M257 (Fig. 3*E*). Again, T cells transduced with 3A1, 9D2, and 1G4 responded comparably to one another, and with higher sensitivity than did those transduced with 5G6 and 4A2. TCR-transduced T cells did not respond to the M257 line lacking HLA-A*02:01. Finally, in vitro cytotoxicity tracked closely with cytokine release: T cells expressing 9D2 or 3A1 killed A2$^+$M257 tumor cells most efficiently, followed by T cells transduced with 1G4, 5G6, and, least efficiently, 4A2 (Fig. 3*F*).

To enable evaluation of TCR function in a tumor xenograft model, we engineered the PC-3 human prostate cancer cell line to express NY-ESO-1 and HLA-A*02:01 and then verified that this line elicited functional responses from TCR-transduced T cells in an antigen-dependent and MHC-restricted manner (*SI Appendix,* Fig. S2*A*). The relative responses to A2$^+$NY$^+$PC-3 from our panel of NY-ESO-1–reactive TCRs were consistent with those elicited by A2$^+$M257 (Fig. 3*E* and *SI Appendix,* Fig. S2*B*). Based on these results, we selected 1G4, 3A1, and 9D2 muTCRs for further functional characterization in vivo. We transduced activated human PBMCs with a vector encoding each murinized TCR and a transduction marker [low-affinity nerve growth factor receptor (LNGFR)] (Fig. 4*A*). We sorted transduced (CD3$^+$LNGFR$^+$) T cells (*SI Appendix,* Fig. S2*C*) and retroorbitally i.v. injected these T cells into irradiated NOD/SCID/γc$^{-/-}$ (NSG) mice preinoculated with PC-3/HLA-A2 (control) and PC-3/HLA-A2/NYESO (target) tumors on opposing flanks (Fig. 4*B*). We then monitored T cell engraftment and tumor size until the conclusion of the experiment 2 wk after T cell injection.

T cells transduced with 1G4 or 9D2 TCRs persisted or minimally expanded in the peripheral blood, while 3A1-transduced T cells expanded significantly (Fig. 4 *C* and *D*). By contrast, T cells transduced only with LNGFR contracted over the course

Fig. 4. In vivo antitumor efficacy of NY-ESO-1 TCR–engineered human T cells. (*A* and *B*) Schematics of the experimental designs to (*A*) generate NY-ESO-1 TCR–engineered human T cells and to (*B*) study antitumor efficacy of these engineered T cells in an NSG mouse human prostate tumor xenograft model. NSG, immunodeficient NOD/SCID/γc$^{−/−}$ mice. (*C*) Representative flow cytometry plots characterizing engineered human T cells present in the peripheral blood of experimental mice on day 14 after adoptive T cell transfer. (*D*) Time course showing persistence of engineered human T cells (gated as LNGFR$^+$ hCD45$^+$) in the peripheral blood of experimental mice. (*E* and *F*) Mean fluorescence intensity measurements for (*E*) murine TCR and (*F*) HLA-A2/NYESO dextramer for engineered human T cells in the peripheral blood of experimental mice on day 14 after adoptive T cell transfer. (*G* and *H*) Measurements of cross-sectional area for (*G*) PC-3/HLA-A2 and (*H*) PC-3/HLA-A2/NYESO tumors. (*I*) Immunohistology images showing representative tumor sections. CD3$^+$ cells are stained in red. (Scale bars: *Upper*, 500 μm; *Lower*, 50 μm.) (*J*) Percentage of CD3$^+$ cell area over whole tumor section area. Representative of two experiments. Data are presented as the mean ± SEM (*n* = 4–5). ns, not significant; *$P < 0.05$, **$P < 0.01$, ***$P < 0.001$, ****$P < 0.0001$, by one-way ANOVA.

of the experiment, suggesting the expansion of TCR-transduced T cells was antigen-driven. The expression level of murine TCRβ was stable over the experimental time course and comparable between T cells transduced with different murinized TCRs (Fig. 4 *C* and *E*). The respective staining levels of each TCR-transduced T cell cohort with A*02:01/NY$_{157–165}$ dextramer$^+$ were also stable over time, but, as expected from results in vitro, were significantly different between TCRs. Approximately 90% of

human T cells transduced with 1G4 or 3A1 were dextramer[+] with high MFI. By contrast, only ~1% of 9D2-transduced T cells were dextramer[+] and the MFI of staining was not significantly different from LNGFR-transduced controls (Fig. 4 *C* and *F*). Nonetheless, T cells transduced with 1G4, 3A1, or 9D2 reduced tumor size comparably and in an antigen-specific manner, while LNGFR-transduced T cells failed to control tumor growth (Fig. 4 *G* and *H*).

At the conclusion of the experiment, we killed the mice and analyzed tumors for T cell infiltration by immunohistochemistry. Immunohistochemical staining revealed antigen-specific T cell infiltration only into target tumors in all cohorts receiving TCR-transduced T cells (Fig. 4 *I* and *J*). Infiltration was significantly

higher in mice receiving 3A1-transduced T cells relative to mice receiving 1G4- or 9D2-transduced T cells.

Functional Characterization of NY-ESO-1–Specific TCRs Restricted on HLA-B and HLA-C Alleles. The majority of immunotherapies targeting NY-ESO-1 have focused on the A2-restricted $NY_{157-165}$ epitope. To enable broader application of NY-ESO-1–targeted immunotherapies, we cloned TCRs from four non-A2-restricted T cell clones and verified NY-ESO-1 reactivity for three of these in transfected CD3^{+} 293T (Fig. 2*D*). The fourth TCR—9G2, cloned from $Cw3/NY_{92-100}$-reactive T cells—did not impart specificity for $Cw3/NY_{92-100}$ on transduced Jurkat T cells even with coexpressed CD8 (Fig. 5 *A* and *B*) and was not studied
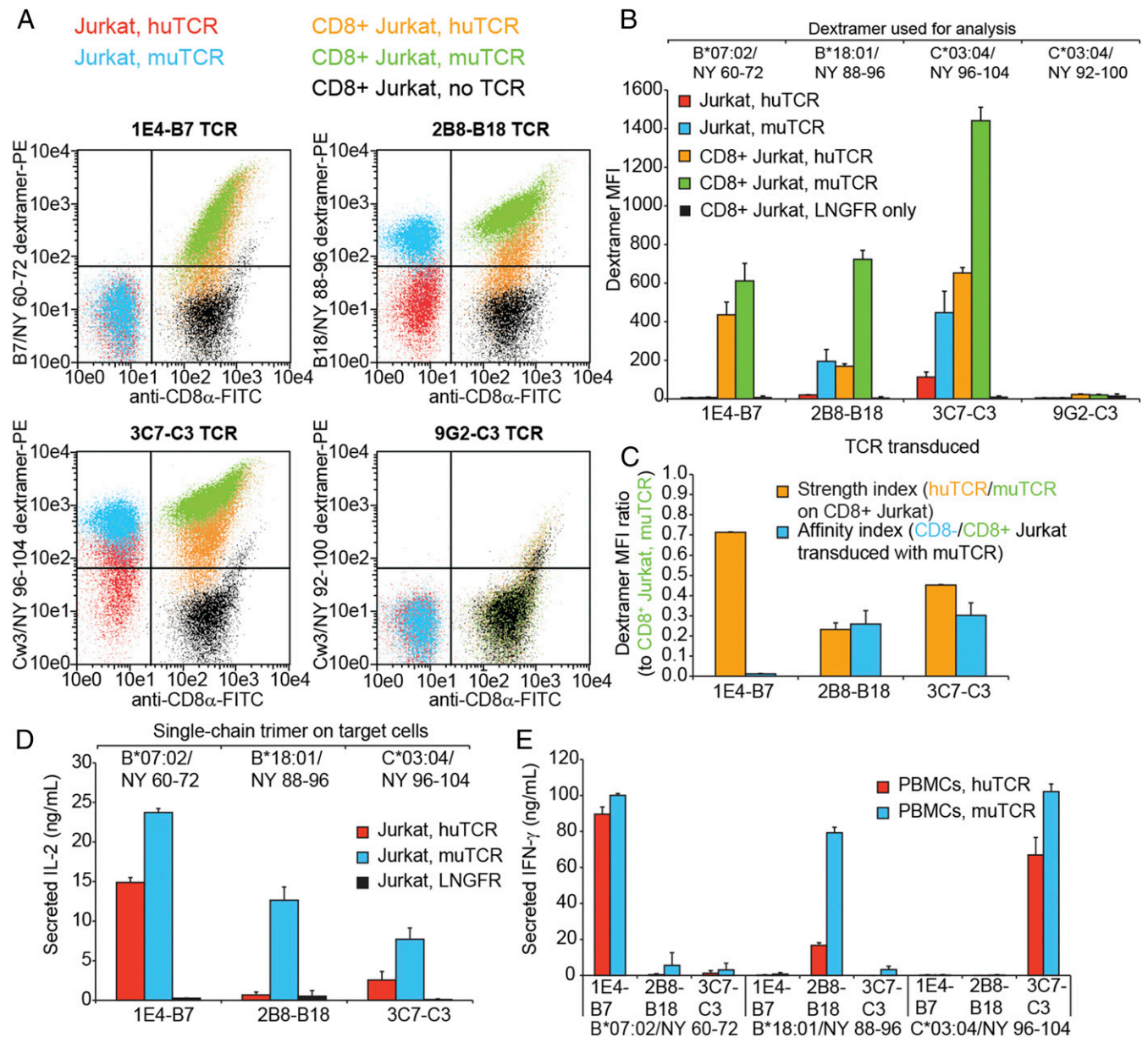
Fig. 5. Function of NY-ESO-1–specific TCRs restricted on MHC alleles other than HLA-A2. (*A*) Overlay of representative flow cytometry plots comparing specified dextramer binding by Jurkat and CD8^{+} Jurkat cells expressing novel TCRs with human or murine constant domains. (*B*) Indicated dextramer binding mean fluorescence intensity measurements from two independent experiments as in *A*. (*C*) Ratio of respective dextramer binding mean fluorescent intensity measurements from two independent experiments in *B*. (*D* and *E*) ELISA measuring (*D*) secretion of IL-2 from TCR-transduced Jurkat cells or (*E*) secretion of IFN-γ from TCR-transduced PBMCs following 48-h coincubation with K562 target cells expressing indicated single-chain trimer. Experiments were repeated three times, each with two technical replicates. Means ± SD for a representative experiment are shown.

further. Comparisons of dextramer binding by the three validated TCRs expressed in Jurkat or CD8$^+$ Jurkat as human or murine TCRs revealed differences in strength and affinity (Fig. 5 A–C). The B7/NY$_{60-72}$-specific 1E4 TCR exhibited high strength but low affinity, expressing comparably on the Jurkat cell surface as either a huTCR or a muTCR but binding dextramer only in the presence of CD8$^+$. Dextramer binding to these CD8$^+$, 1E4-transduced cells was steeply dependent on the level of CD8 expressed. By contrast, the B18/NY$_{88-96}$-specific 2B8 TCR bound dextramer in the absence of CD8$^+$, but binding was substantially higher for the murinized TCR. Finally, the Cw3/NY$_{96-104}$-specific 3C7 TCR exhibited intermediate strength of surface expression and an affinity index comparable to 2B8.

These differences in TCR strength and affinity were reflected in functional assays. For all three TCRs, murinization of the TCR constant regions increased production of IL-2 from TCR-transduced Jurkat cells coincubated with cognate target cells. However, this increase was only 1.6- and 3.0-fold over the respective fully human TCRs for 1E4 and 3C7 but was 18.6-fold for 2B8, consistent with the latter's lower strength (Fig. 5D). In peptide titration assays, 1E4 TCR imparted lower sensitivity for cognate peptide on transduced CD8$^+$ T cells than did 3C7 or 2B8 (*SI Appendix*, Fig. S1 *C–E*), consistent with the presumed lower affinity of 1E4 based on its strictly CD8-dependent dextramer binding.

Primary PBMCs transduced with each TCR responded to the presentation of NY-ESO-1–derived epitopes in a peptide-specific and MHC-restricted manner (Fig. 5E). As such, we expect that TCR gene therapies employing NY-ESO-1–specific TCRs restricted on multiple MHCs can be applied more broadly across patient haplotypes and will be more robust toward tumor evasion via loss of heterozygosity at the MHCI locus. To test this, we transduced NY-ESO-1–expressing human cancer cells with HLA-A2 or HLA-B7. We then coincubated one or both of these tumor targets with human T cells transduced with A2-restricted 3A1 TCR, with T cells transduced with B7-restricted 1E4 TCR, or with a mixture of 3A1- and 1E4-transduced T cells (Fig. 6). As expected, combination targeting using a mixture of 3A1- and 1E4-transduced T cells enabled recognition of tumor cell populations expressing both MHC alleles or either MHC allele alone (Fig. 6 *A* and *B*). By contrast, T cells targeting a single NY-ESO-1 epitope did not respond to NY-ESO-1–expressing tumor cells that lacked the cognate MHC allele. Moreover, when tumor targets comprised a mixture of cells expressing different MHC alleles (simulating tumor heterogeneity arising from haploinsufficiency), T cells targeting both NY-ESO-1 epitopes killed tumor cells more completely than did T cells targeting either single epitope (Fig. 6 *C* and *D*).

Discussion

T cell-mediated immunotherapies are making clinical inroads for previously refractory cancers. Two of the most successful immunotherapy modalities are checkpoint blockade and adoptive transfer of cancer-specific T cells. Checkpoint blockade elicits better clinical responses as tumor mutational burden increases (39–41), suggesting that nonsynonymous mutations go undetected by the immune system unless, fortuitously, they generate neoepitopes that are presented by the patient's complement of MHC molecules. This interpretation is bolstered by the recent finding that checkpoint blockade results in higher overall survival for melanoma patients who are heterozygous at the HLA-A, HLA-B, and HLA-C loci and thus present a more diverse array of epitopes than those who are homozygous at one or more of these MHCI loci (42). The importance of a diversely targeted antitumor immune response is likewise supported by results from adoptive T cell therapy, which show that loss of heterozygosity is a mechanism by which tumors can evade monospecific immune recognition while continuing to express an otherwise immunogenic antigen (43). Thus, a prominent narrative emerging from these studies is that diverse

targeting of multiple epitopes presented by multiple MHC alleles is desirable for successful immunotherapy. A second takeaway is that targeting multiple epitopes derived from a tumor-specific public antigen may be a promising alternative to targeting neo-epitopes in cancers with low mutational burden.

It has proven difficult to identify public tumor-associated antigens that mediate tumor regression without also manifesting serious morbidity or deaths resulting from on-target, off-tumor T cell reactivity. We chose to focus on NY-ESO-1 as a public antigenic target based on the criteria that it (*i*) is expressed exclusively in cancer cells and immunologically privileged germ cells; (*ii*) is expressed in many patients across various tumor types; (*iii*) harbors high-affinity ligands for multiple common MHC alleles; (*iv*) is well-vetted, having yielded objective responses in patients across several tumor types without specificity-related adverse events; and (*v*) is yet underexploited, as the majority of studies have focused on mobilizing T cell responses solely against the A2-restricted NY-ESO-1$_{157-165}$ epitope.

We employed an antigen-specific expansion protocol to isolate NY-ESO-1–reactive T cells from the peripheral blood of patients with metastatic melanoma. Using this approach, we cloned several HLA-A2–restricted TCRs and compared them in terms of their strength of surface expression, affinity (i.e., dependence of target binding on CD8), and function (antigen-induced cytokine release and tumor target killing). From four candidates, we identified two that recognized and killed NY-ESO-1–expressing cancer cells as well or better than the clinically employed 1G4 TCR. This expansion-based approach to TCR candidate identification is ideally suited for targeting public epitopes because the speed of isolation is not a critical parameter; once identified, these TCRs can be used as off-the-shelf targeting receptors for any patient expressing the requisite MHC allele. Antigen-specific expansion of neoantigen-reactive T cells from peripheral blood has also been demonstrated (44, 45). However, on-demand isolation of private neoepitope-targeted TCRs will require more rapid approaches than that used here (e.g., direct capture of antigen-specific T cells from blood or expansion protocols optimized for rapidity). As the release of IFN-γ is strongly correlated with cytotoxicity (46), candidate evaluation can be accelerated by using IFN-γ release as a surrogate for more involved tumor xenograft assays.

One of the HLA-A2/NY-ESO-1–reactive TCRs isolated—9D2—exhibited poor staining with cognate multimer but high functional avidity toward cognate antigen-presenting target cells. This is consistent with the observation that multimer staining underestimates functional T cell subsets (47) and may be explained by the higher-affinity threshold for multimer binding relative to that for T cell activation (48). However, another isolated A2-restricted TCR—4A2—exhibited robust multimer staining but poor function in cell-based assays, seemingly at odds with this affinity threshold explanation. While we do not have an explanation for this latter result, both results caution against relying too much on multimer staining when down-selecting immunotherapy candidates.

The HLA-A*02:01 allele is the most prevalent MHCI allele in Caucasian (45%) and Hispanic (41%) US populations, but it is less common among Asian (15%) and African (16%) US populations (2). These latter populations would be particularly well-served by expanding the targeting of TCR gene therapies beyond HLA-A2 to a more expansive panel of targetable MHC alleles. In addition to HLA-A2–restricted TCRs, we isolated and functionally characterized NY-ESO-1–specific TCRs restricted on various HLA-B and HLA-C alleles. In doing so, we demonstrated in principle that TCR gene therapy can be extended to a greater subset of patients/haplotypes and that, when used in combination, TCRs recognizing multiple epitopes from the same antigen can more robustly kill tumors with heterogeneous MHC expression (e.g., resulting from somatic loss of heterozygosity).
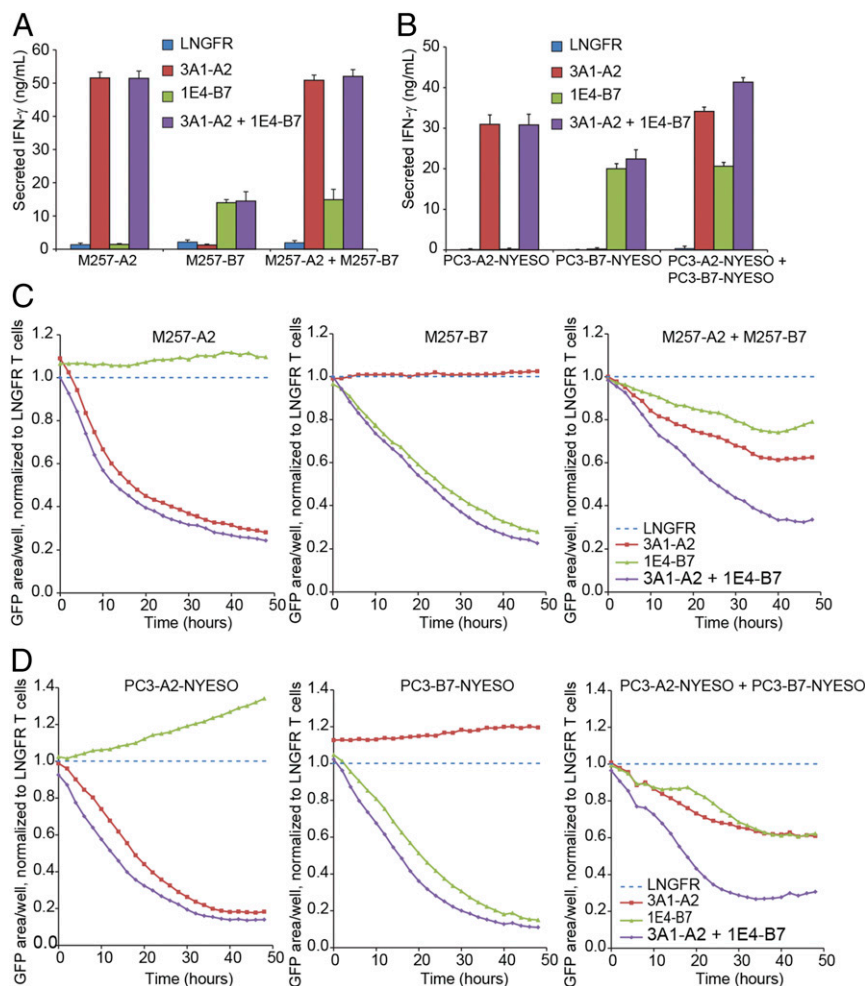
Fig. 6. Targeting NY-ESO-1 epitopes restricted on multiple MHC alleles broadens the application of TCR gene therapy and makes it robust toward loss of heterozygosity at the MHC locus. (*A–D*) T cells transduced with LNGFR only, A2-restricted 3A1 TCR, or B7-restricted 1E4 TCR—or a 1:1 mixture of 3A1-transduced and 1E4-transduced T cells—were coincubated for 48 h with HLA-A2$^+$eGFP$^+$ target cells, HLA-B7$^+$eGFP$^+$ target cells, or a 1:1 target cell mixture. (*A* and *B*) ELISA measuring secretion of IFN-γ from TCR-transduced PBMCs following 48-h coincubation with (*A*) M257 or (*B*) PC-3 tumor cell lines engineered to express eGFP and HLA-A*02:01 or HLA-B*07:02. PC-3 lines were additionally engineered to express NY-ESO-1. M257 lines express endogenous NY-ESO-1. Experiments were repeated three times, each with four or eight replicates. Means ± SD for a representative experiment are shown. (*C* and *D*) T cell-mediated killing of (*C*) M257 and (*D*) PC-3 tumor cell line derivatives measured over time using IncuCyte live-cell analysis. Total green object area (indicative of tumor cell density) at each time point measured over 48 h was normalized for each treatment relative to treatment with LNGFR-transduced T cells. Experiments were repeated three times, each with four or eight replicates. Results from a representative eight-replicate experiment are shown.

Over 80% of people across ethnic groups express at least one allele from three MHCI supertypes (A2, A3, and B7, two of which were represented here) and >99% of people express at least one allele from nine MHCI supertypes (49). Therefore, obtaining a panel of public antigen-specific TCR reagents that enable comprehensive application of TCR gene therapy is a finite and surmountable challenge.

Materials and Methods

Materials. Peptides were purchased from Anaspec, Thermo Fisher Scientific, and Mimotopes. Fluorescent antibodies and 7-AAD used for flow cytometry were purchased from BD Biosciences, BioLegend, or eBioscience. Fluorescent peptide–MHC multimers were purchased from TCMetrix or prepared in-house as described (50) from biotinylated monomers [obtained from NIH Tetramer Core, or expressed heterologously in *Escherichia coli*, refolded, and biotinylated in-house as described (51)]. Primers were purchased from Integrated DNA Technologies. KOD polymerase master mix and polybrene were purchased from EMD Millipore. Sequencing was performed by Retrogen Inc. Anti-CD3 (OKT3) and anti-CD28 (CD28.2) activating antibodies were purchased from eBioscience. Cytokines were purchased from Peprotech, Inc. BioT transfection reagent was purchased from Bioland Scientific. Cell culture

media, antibiotics, and FBS were purchased from Corning. Human AB serum was purchased from Omega Scientific. Poly-L-lysine and PHA-L (phytohemagglutinin-L) were purchased from Sigma.

Cells. Cell lines (293T/17, Jurkat E6-1, and K562) were purchased from the American Type Culture Collection. The 293T cells were grown in DMEM supplemented with antibiotics (penicillin/streptomycin) and 10% (vol/vol) FBS. Jurkat and K562 cells were grown in RPMI medium 1640 supplemented with antibiotics, 10% (vol/vol) FBS, 10 mM Hepes, 50 μM β-mercaptoethanol, 1× MEM NEAA, and 1 mM sodium pyruvate. The cells were split every 2–3 d to maintain adherent cells subconfluently or nonadherent cells at a density of <10^6 cells/mL Jurkat and K562 cells were transduced with nonreplicative viral vectors, analyzed by flow cytometry, and used directly in cell assays or sorted by FACS to establish derivative cell lines as indicated. Primary human PBMCs used in functional assays were purchased from the CFAR Virology Core Laboratory at the University of California, Los Angeles (UCLA) AIDS Institute, stimulated, transduced, and cultured as previously described (52). T cells were grown from PBMCs in T cell medium (AIM-V medium supplemented with 5% heat-inactivated human AB serum, 55 μM β-mercaptoethanol, and 4 mM L-glutamine) with freshly added cytokines. All cells were grown and assayed at 37 °C with 5% atmospheric CO$_2$.

Generation and Culture of NY-ESO-1–Specific CD8$^+$ T Lymphocyte Clones. CD8$^+$ T lymphocyte clones specific for epitopes from NY-ESO-1 with various HLA restrictions [157–165/HLA-A*02:01 (53), 60–72/HLA-B*07:02 (21), 88–96/HLA-B*18:01 (23), 92–100/HLA-C*03:04 (54), 96–104/HLA-C*03:04 (22), and 124–133/HLA-C*03:04 (22)] were generated from HLA-typed patients with melanoma. All selected patients had grade III/IV metastatic melanoma and previously documented NY-ESO-1 responses to relevant T lymphocyte epitopes ex vivo (55). Patient PBMCs were stimulated in the presence of 1 μM pooled peptides (Mimotopes), comprising 28 × 18-mers overlapping by 12 aa, collectively spanning the NY-ESO-1 protein sequence and then cultured for 10 d in the presence of 25 IU/mL IL-2 (Peprotech).

On day 10, cells were restimulated with 1 μM of each individual peptide in the presence of brefeldin A and activation of CD8$^+$ T cells in response to each peptide was determined by intracellular cytokine stain. Briefly, cells were labeled with live/dead fixable violet stain (Invitrogen) according to the manufacturer's instructions then incubated with antibodies against CD3 and CD8 for 15 min at 4 °C. Samples were washed and fixed with fix/permeabilization reagent (BD Biosciences) for 20 min at 4 °C. Cells were stained with anti–IFN-γ (eBiosciences) in permeabilization/wash solution (BD Biosciences) for 25 min at 4 °C. The gating strategy was SSC/LD$^-$; CD3$^+$/CD8$^+$; CD8$^+$/IFN-γ$^+$. Data from at least 100,000 stained cells were acquired on a FACSCanto and analyzed with FlowJo software. Data collection and analysis was in accordance with the Minimal Information About T cell Assays guidelines (56).

NY-ESO-1–reactive T cells were expanded in the presence of their identified cognate 9–10-mer epitope and then labeled with a fluorescent tetramer comprising the relevant peptide and HLA molecule (TCMetrix) and single-cell-sorted using a MoFlo cell sorter. Clones were reexpanded with pooled, allogeneic healthy donor PBMC as feeder cells, 1 μg/mL PHA-L, and 600 IU/mL IL-2 (Cetus). After ∼20 d, 1–10 × 10^3 clones were restimulated in the presence of allogeneic PBMC as feeder cells, PHA-L, and IL-2, as described above. Clone specificity was confirmed by tetramer staining.

T lymphocyte clones/lines were cultured in RPMI 1640 media supplemented with 2 mM Glutamax, 100 IU/mL penicillin, 100 μg/mL streptomycin, 20 mM Hepes, 1% nonessential amino acids, 1 mM sodium pyruvate, 55 μM β-mercaptoethanol, and 10% human serum (TCRPMI). IL-2 (100 IU/mL) was added and replaced every 3 d.

Cloning TCR Constructs. Single NY-ESO-1–reactive T cells were sorted for antigenic specificity on a FACS Aria II and were lysed by freeze–thaw in the presence of RNase inhibitor. Novel TCR variable genes were cloned from single, sorted T cells using a custom panel of human TCR variable region-specific primers with the Qiagen OneStep RT-PCR kit, followed by a nested PCR amplification step. Amplified variable genes were integrated via assembly PCR and restriction enzyme-mediated cloning into a TCR expression cassette with either human or mouse TCR constant domains and a 2A ribosomal skipping peptide linking the alpha and beta genes. A P2A-linked gene encoding a truncated version of the LNGFR was also included in the cassette as an independent transfection/transduction marker. Antigenic specificity and MHC restriction of cloned TCRs were evaluated in 293T cells cotransfected with TCR and CD3 genes, as previously described (52).

Evaluation of TCR Export and Dextramer Binding on Jurkat T Cells. Jurkat T cells were transduced with MSGV-based retroviruses encoding each novel TCR in the format LNGFRΔ-P2A-TCRα-F2A-TCRβ. Viruses were produced in 293T cells as described (52). For transduction, Jurkat T cells were centrifuged (1,350 × *g* for 90 min at 30 °C) with unconcentrated viral supernatants supplemented with 5 μg/mL polybrene. TCR-transduced Jurkat cells were stained with cognate pMHC dextramer for 15 min at room temperature and then costained with antibodies against LNGFR and CD8α for 15 min at 4 °C. Stained cells were analyzed by flow cytometry using a FACSCanto analyzer. Data shown are gated on LNGFR$^+$ (transduced) cells. Transduction efficiency was >95%.

PBMC Activation and Transduction. Primary human PBMCs were purchased from the CFAR Virology Core Laboratory at the UCLA AIDS Institute. The same PBMC donor was used in all reported experiments. Primary human PBMCs were transduced with retroviruses encoding novel TCRs as described (52). Briefly, 2 d before viral transduction, 1–2 × 10^6 total thawed PBMCs were activated per well in 24-well plates with plate-coated anti-CD3 (clone OKT3), T cell medium containing 1 μg/mL soluble anti-CD28 (clone CD28.2), and 300 U/mL IL-2. After 48 h of activation, the majority of the medium was replaced with unconcentrated retroviral supernatant supplemented with 10 μg/mL polybrene and cells were centrifuged for 90 min at 1,350 × *g* at 30 °C. Following spinfection, the majority of retroviral supernatant was replaced with fresh medium containing 300 U/mL IL-2 and 1 μg/mL anti-CD28. The transduction was repeated 24 h later, after which the cells were washed with 1× PBS

and then returned to fresh medium containing final 300 U/mL IL-2 and cultured for an additional 3–4 d before being used in antigenic stimulation assays. One day before or on the day of coculturing, PBMCs were analyzed by FACS for assessment of expression levels for LNGFR, TCR, and/or pMHC multimer binding.

Functional Coculture Assays: Cytokine ELISA. When Jurkat T cells were used as effectors, cocultures were performed in RPMI supplemented with 10% FBS, 100 IU/mL penicillin, 100 μg/mL streptomycin, and 4 mM L-glutamine. Effector cells (50,000 TCR-transduced Jurat T cells) were coincubated with target cells (50,000 K562 cells transduced with cognate or control single-chain trimers) in 96-well flat-bottom plates. Supernatants from duplicate wells were collected 44–48 h postcoculturing and analyzed by ELISA as described below.

When primary PBMCs were used as effectors, cocultures were performed in T cell media containing 300 U/mL IL-2. Effector cells (50,000 TCR-transduced PBMCs) were coincubated with target cells (50,000 M257, PC-3, or K562 cells) in 96-well flat-bottom plates. In some experiments target cells were pulsed with peptide. Supernatants from two eightfold replicate wells for each condition were collected 44–48 h postcoculturing and analyzed by ELISA as described below.

For experiments in which target cells were titrated with pulsed peptide, lyophilized peptides were dissolved to 10 mM in DMSO and then further diluted in water to 2 mM working stocks. At point of use, the 2 mM stock was diluted to 250 μM in cell media and then fivefold serially diluted from 250 μM down to 3.2 nM. Target cells were pulsed by adding 25 μL of each serial dilution per well on a 96-well U-bottom plate, followed by addition of 50,000 target cells in 100 μL media, yielding the final peptide concentration ranging from 50 μM to 0.64 nM. Cells were pulsed with peptides for 2 h at 37 °C, diluted with 100 μL of media per well at the end of incubation, and centrifuged, and the supernatant was removed. The cells were washed with 200 μL of media and then resuspended in 100 μL of media. Fifty thousand PBMCs prepared in 100 μL of media were then added to each well for coculturing.

In general, ELISA results were converted to concentration (nanograms per milliliter) by interpolation relative to a standard curve and concentrations from replicate ELISAs were averaged. Supernatants were diluted 50- to 100-fold for ELISA analysis. Occasionally, higher dilutions were required to place signal within the range of the standard curve. All reagents for ELISA analyses were from BD Biosciences: OptEIA Reagent Set B (550534) was used for diluent and washes and OptEIA human IFN-γ ELISA kit (555142) and OptEIA human IL-2 ELISA kit (555190) were used for measuring IFN-γ and IL-2 release, respectively.

Functional Coculture Assays: IncuCyte Cell Killing Assay. Before coculture for IncuCyte killing assays, a 96-well flat-bottom plate was coated with 100 μL of 0.001% poly-L-lysine in PBS for 1 h at 37 °C, washed two times with 200 μL PBS each, and air-dried briefly. Target cells were added and allowed to settle at room temperature for 3 h before the effector cells were added. Cocultures typically employed 25,000 PBMCs and 25,000 target cells per well of a 96-well plate. In assays where multiple effector populations (bearing different TCRs) or multiple targets (bearing different MHC) were mixed, 25,000 of each cell type was used to yield a total of 75,000 or 100,000 cells per well (for single/mixed or mixed/mixed, respectively). The total volume for all wells was adjusted to 200 μL. Total green object area (square micrometers per well) was quantified and its disappearance interpreted as killing of the GFP$^+$ target cells. Cells were imaged at two positions per well every 2 h and these two images were added together for one data point. Data points obtained from four to eight replicate cocultures for each effector/target combination were used to plot graph curves and to calculate SD.

Animals. NOD.Cg-PrkdcSCIDIL-2rgtm1Wjl/SzJ (NOD/SCID/IL-2Rg$^{-/-}$, NSG) mice were purchased from The Jackson Laboratory and maintained in the animal facilities at UCLA. Adult (16 wk old) male mice were used for in vivo tumor challenge experiments. All animal experiments were approved by the Institutional Animal Care and Use Committee of UCLA.

Human Prostate Tumor Xenograft Mouse Model. For xenograft tumor implantation, 10 × 10^6 PC-3/HLA-A2 cells (PC-3 cell line overexpressing HLA-A2) were s.c. injected on one flank of each mouse and 10 × 10^6 PC-3/HLA-A2/NYESO cells (PC-3 cell line overexpressing HLA-A2 and NYESO) were s.c. injected on the other flank. Mice were allowed to develop solid tumors over the course of 1 wk. On day 8 after tumor injection, mice were irradiated (100 rad) and then retroorbitally i.v. injected with 8 × 10^6 purified T cells that were engineered to express LNGFR only or together with a NY-ESO-1–specific TCR (1G4, 3A1, or 9D2). Mice were bled on days 3, 7, 10, and 14 for flow cytometry analysis. On day 14, mice were killed and tumors were collected for immunohistology analysis.

Immunohistology. Solid tumors dissected out from the experimental mice were fixed in 10% neutral-buffered formalin and embedded in paraffin for sectioning (4-mm thickness), followed by H&E staining or antibody staining (for human CD3ε) by using standard procedures (UCLA Translational Pathology Core Laboratory). The sections were imaged using an Olympus BX51 upright microscope equipped with an Optronics Macrofire CCD camera (AU Optronics) at 4× and 40× magnifications. The images were analyzed by using Optronics PictureFrame software (AU Optronics) and ImageJ software (version 1.51J8). With ImageJ human CD3 antibody-stained slides were quantified by measuring CD3$^+$ area through setting color threshold. Parameters used are as follows: thresholding method: default; threshold color: red; color space: HSB; brightness: 168–215.

Statistical Analysis. Statistical analysis of tumor xenograft experiments was performed with one-way ANOVA followed by Tukey's multiple comparison test. Data are presented as the mean ± SEM. $P < 0.05$ was considered significant. ns, not significant; *$P < 0.05$; **$P < 0.01$; ***$P < 0.001$; ****$P < 0.0001$. All statistical analyses were performed with GraphPad PRISM software (version 6.0).

1. Robinson J, et al. (2015) The IPD and IMGT/HLA database: Allele variant databases. *Nucleic Acids Res* 43:D423–D431.
2. González-Galarza FF, et al. (2015) Allele frequency net 2015 update: New features for HLA epitopes, KIR and disease and HLA adverse drug reaction associations. *Nucleic Acids Res* 43:D784–D788.
3. Johnson LA, et al. (2006) Gene transfer of tumor-reactive TCR confers both high avidity and tumor reactivity to nonreactive peripheral blood mononuclear cells and tumor-infiltrating lymphocytes. *J Immunol* 177:6548–6559.
4. Schumacher TN, Schreiber RD (2015) Neoantigens in cancer immunotherapy. *Science* 348:69–74.
5. Bethune MT, Joglekar AV (2017) Personalized T cell-mediated cancer immunotherapy: Progress and challenges. *Curr Opin Biotechnol* 48:142–152.
6. Morgan RA, et al. (2006) Cancer regression in patients after transfer of genetically engineered lymphocytes. *Science* 314:126–129.
7. Johnson LA, et al. (2009) Gene therapy with human and mouse T-cell receptors mediates cancer regression and targets normal tissues expressing cognate antigen. *Blood* 114:535–546.
8. Parkhurst MR, et al. (2011) T cells targeting carcinoembryonic antigen can mediate regression of metastatic colorectal cancer but induce severe transient colitis. *Mol Ther* 19:620–626.
9. Morgan RA, et al. (2010) Case report of a serious adverse event following the administration of T cells transduced with a chimeric antigen receptor recognizing ERBB2. *Mol Ther* 18:843–851.
10. Morgan RA, et al. (2013) Cancer regression and neurological toxicity following anti-MAGE-A3 TCR gene therapy. *J Immunother* 36:133–151.
11. Anonymous (2013) Do no harm. *Nat Biotechnol* 31:365.
12. Jorritsma A, et al. (2007) Selecting highly affine and well-expressed TCRs for gene therapy of melanoma. *Blood* 110:3564–3572.
13. Chen YT, et al. (1997) A testicular antigen aberrantly expressed in human cancers detected by autologous antibody screening. *Proc Natl Acad Sci USA* 94:1914–1918.
14. Goydos JS, Patel M, Shih W (2001) NY-ESO-1 and CTp11 expression may correlate with stage of progression in melanoma. *J Surg Res* 98:76–80.
15. Sharma P, et al. (2003) Frequency of NY-ESO-1 and LAGE-1 expression in bladder cancer and evidence of a new NY-ESO-1 T-cell epitope in a patient with bladder cancer. *Cancer Immun* 3:19.
16. Li M, et al. (2005) Expression profile of cancer-testis genes in 121 human colorectal cancer tissue and adjacent normal tissue. *Clin Cancer Res* 11:1809–1814.
17. Gure AO, et al. (2005) Cancer-testis genes are coordinately expressed and are markers of poor outcome in non-small cell lung cancer. *Clinical Cancer Res* 11:8055–8062.
18. Jungbluth AA, et al. (2001) Monophasic and biphasic synovial sarcomas abundantly express cancer/testis antigen NY-ESO-1 but not MAGE-A1 or CT7. *Int J Cancer* 94:252–256.
19. Aung PP, et al. (2014) Expression of New York esophageal squamous cell carcinoma-1 in primary and metastatic melanoma. *Hum Pathol* 45:259–267.
20. Ademuyiwa FO, et al. (2012) NY-ESO-1 cancer testis antigen demonstrates high immunogenicity in triple negative breast cancer. *PLoS One* 7:e38783, and erratum (2012) 7:10.1371/annotation/5cdf6105-2a52-497a-86b3-db8f4a4e439c.
21. Ebert LM, et al. (2009) A long, naturally presented immunodominant epitope from NY-ESO-1 tumor antigen: Implications for cancer vaccine design. *Cancer Res* 69:1046–1054.
22. Jackson H, et al. (2006) Striking immunodominance hierarchy of naturally occurring CD8+ and CD4+ T cell responses to tumor antigen NY-ESO-1. *J Immunol* 176:5908–5917.
23. Zhao RY, et al. (2012) A novel HLA-B18 restricted CD8+ T cell epitope is efficiently cross-presented by dendritic cells from soluble tumor antigen. *PLoS One* 7:e44707.
24. Robbins PF, et al. (2011) Tumor regression in patients with metastatic synovial cell sarcoma and melanoma using genetically engineered lymphocytes reactive with NY-ESO-1. *J Clin Oncol* 29:917–924.
25. Robbins PF, et al. (2015) A pilot trial using lymphocytes genetically engineered with an NY-ESO-1-reactive T-cell receptor: Long-term follow-up and correlates with response. *Clinical Cancer Res* 21:1019–1027.
26. Rapoport AP, et al. (2015) NY-ESO-1-specific TCR-engineered T cells mediate sustained antigen-specific antitumor effects in myeloma. *Nat Med* 21:914–921.
27. Klippel ZK, et al. (2014) Immune escape from NY-ESO-1-specific T-cell therapy via loss of heterozygosity in the MHC. *Gene Ther* 21:337–342.
28. Zhao Y, et al. (2007) High-affinity TCRs generated by phage display provide CD4+ T cells with the ability to recognize and kill tumor cell lines. *J Immunol* 179:5845–5854.
29. Cameron BJ, et al. (2013) Identification of a Titin-derived HLA-A1-presented peptide as a cross-reactive target for engineered MAGE A3-directed T cells. *Sci Transl Med* 5:197ra103.
30. Linette GP, et al. (2013) Cardiovascular toxicity and titin cross-reactivity of affinity-enhanced T cells in myeloma and melanoma. *Blood* 122:863–871.
31. Andreatta M, Nielsen M (2016) Gapped sequence alignment using artificial neural networks: Application to the MHC class I system. *Bioinformatics* 32:511–517.
32. Wooldridge L, et al. (2005) Interaction between the CD8 coreceptor and major histocompatibility complex class I stabilizes T cell receptor-antigen complexes at the cell surface. *J Biol Chem* 280:27491–27501.
33. Aleksic M, et al. (2012) Different affinity windows for virus and cancer-specific T-cell receptors: Implications for therapeutic strategies. *Eur J Immunol* 42:3174–3179.
34. Sommermeyer D, et al. (2006) Designer T cells by T cell receptor replacement. *Eur J Immunol* 36:3052–3059.
35. Klausner RD, Lippincott-Schwartz J, Bonifacino JS (1990) The T cell antigen receptor: Insights into organelle biology. *Annu Rev Cell Biol* 6:403–431.
36. Cohen CJ, Zhao Y, Zheng Z, Rosenberg SA, Morgan RA (2006) Enhanced antitumor activity of murine-human hybrid T-cell receptor (TCR) in human lymphocytes is associated with improved pairing and TCR/CD3 stability. *Cancer Res* 66:8878–8886.
37. Robbins PF, et al. (2008) Single and dual amino acid substitutions in TCR CDRs can enhance antigen-specific T cell functions. *J Immunol* 180:6116–6131.
38. Hansen T, Yu YY, Fremont DH (2009) Preparation of stable single-chain trimers engineered with peptide, beta2 microglobulin, and MHC heavy chain. *Curr Protoc Immunol* Chap 17:Unit17.5.
39. Snyder A, et al. (2014) Genetic basis for clinical response to CTLA-4 blockade in melanoma. *N Engl J Med* 371:2189–2199.
40. Van Allen EM, et al. (2015) Genomic correlates of response to CTLA-4 blockade in metastatic melanoma. *Science* 350:207–211.
41. Rizvi NA, et al. (2015) Cancer immunology. Mutational landscape determines sensitivity to PD-1 blockade in non-small cell lung cancer. *Science* 348:124–128.
42. Chowell D, et al. (2018) Patient HLA class I genotype influences cancer response to checkpoint blockade immunotherapy. *Science* 359:582–587.
43. Tran E, et al. (2016) T-cell transfer therapy targeting mutant KRAS in cancer. *N Engl J Med* 375:2255–2262.
44. Gros A, et al. (2016) Prospective identification of neoantigen-specific lymphocytes in the peripheral blood of melanoma patients. *Nat Med* 22:433–438.
45. Strønen E, et al. (2016) Targeting of cancer neoantigens with donor-derived T cell receptor repertoires. *Science* 352:1337–1341.
46. Ioannidou K, et al. (2017) Heterogeneity assessment of functional T cell avidity. *Sci Rep* 7:44320.
47. Rius C, et al. (2018) Peptide-MHC class I tetramers can fail to detect relevant functional T cell clonotypes and underestimate antigen-reactive T cell populations. *J Immunol* 200:2263–2279.
48. Laugel B, et al. (2007) Different T cell receptor affinity thresholds and CD8 coreceptor dependence govern cytotoxic T lymphocyte activation and tetramer binding properties. *J Biol Chem* 282:23799–23810.
49. Sette A, Sidney J (1999) Nine major HLA class I supertypes account for the vast preponderance of HLA-A and -B polymorphism. *Immunogenetics* 50:201–212.
50. Bethune MT, Comin-Anduix B, Hwang Fu YH, Ribas A, Baltimore D (2017) Preparation of peptide-MHC and T-cell receptor dextramers by biotinylated dextran doping. *Biotechniques* 62:123–130.
51. Toebes M, et al. (2006) Design and use of conditional MHC class I ligands. *Nat Med* 12:246–251.
52. Bethune MT, et al. (2016) Domain-swapped T cell receptors improve the safety of TCR gene therapy. *eLife* 5:e19095.
53. Chen JL, et al. (2000) Identification of NY-ESO-1 peptide analogues capable of improved stimulation of tumor-reactive CTL. *J Immunol* 165:948–955.
54. Gnjatic S, et al. (2000) Strategy for monitoring T cell responses to NY-ESO-1 in patients with any HLA class I allele. *Proc Natl Acad Sci USA* 97:10917–10922.
55. Davis ID, et al. (2004) Recombinant NY-ESO-1 protein with ISCOMATRIX adjuvant induces broad integrated antibody and CD4(+) and CD8(+) T cell responses in humans. *Proc Natl Acad Sci USA* 101:10697–10702.
56. Britten CM, et al. (2012) T cell assays and MIATA: The essential minimum for maximum impact. *Immunity* 37:1–2.

MEDICAL SCIENCES